From dinuclear to tetranuclear zinc complexes through carboxylate donors: structural and luminescence studies†

Matilde Fondo,*[a] Ana M. García-Deibe,[a] Noelia Ocampo,[a] Jesús Sanmartín,[b] Manuel R. Bermejo,[b] Elisabete Oliveira[c] and Carlos Lodeiro[c]

Received (in Montpellier, France) 12th July 2007, Accepted 13th September 2007
First published as an Advance Article on the web 27th September 2007
DOI: 10.1039/b710660b

Carboxylate zinc complexes of general formula $[Zn_2L^x(p\text{-}OOC\text{–}C_6H_4\text{–}CHO)]$, $[Zn_2L^x(o\text{-}OOC\text{–}C_6H_4\text{–}COOH)]$, $[(Zn_2L^x)_2(OOC\text{–}CH_2\text{–}COO)]$, $[(Zn_2L^x)_2(OOC\text{–}CH_2CH_2\text{–}COO)]$ and $[(Zn_2L^x)_2(p\text{-}OOC\text{–}C_6H_4\text{–}COO)]$ (x = 1, 2; H_3L^1 = 2-(2-hydroxyphenyl)-1,3-bis[4-(2-hydroxyphenyl)-3-azabut-3-enyl]-1,3-imidazolidine and H_3L^2 = 2-(5-bromo-2-hydroxyphenyl)-1,3-bis[4-(5-bromo-2-hydroxyphenyl)-3-azabut-3-enyl]-1,3-imidazolidine) were isolated with different solvates. The crystal structures of $[Zn_2L^1(p\text{-}OOC\text{–}C_6H_4\text{–}CHO)]\cdot 2.5DMSO\cdot 2H_2O$, $[(Zn_2L^1)_2(OOC\text{–}CH_2CH_2\text{–}COO)]\cdot 4.25H_2O\cdot 0.75MeOH\cdot 0.5MeCN$, $[(Zn_2L^2)_2(OOC\text{–}CH_2CH_2\text{–}COO)]\cdot 7H_2O\cdot 0.25MeOH$ and $[(Zn_2L^1)_2(p\text{-}OOC\text{–}C_6H_4\text{–}COO)]\cdot 2.5H_2O\cdot MeOH\cdot 6EtOH$ demonstrate that their different nuclearities are a function of the carboxylate donor, with the aldehyde residue remaining uncoordinated in $[Zn_2L^1(p\text{-}OOC\text{–}C_6H_4\text{–}CHO)]\cdot 2.5DMSO\cdot 2H_2O$. The solution studies further support the dissimilar nuclearity of the complexes and agree with a dinuclear nature for those complexes containing *ortho*-phthalate or 4-formylbenzenecarboxylate, and a tetranuclear arrangement when malonate, succinate or terephthalate are used as co-ligands. The ability of both Schiff base ligands to recognize Zn(II) in solution was studied by UV-vis and emission spectroscopies. The luminescent properties of the ligands and their isolated complexes are also discussed in detail.

Introduction

The study of multinuclear metal complexes with low nuclearities is an area of current interest, stimulated by the potential significance of these compounds as building blocks for coordination polymers,[1–6] as catalysts[7] and as models in bioinorganic chemistry.[8–10] Actually, it is well known that many metallobiosites hold two transition metal ions in close proximity, so that the two metal centres cooperate with each other. In past decades, much effort has been devoted to developing ligands with the ability to bind two metal ions, and to permit them to interact and/or assist in their molecular frameworks. Among the various synthetic approaches, the use of dinucleating Schiff base ligands seems to be especially appropriate to modulate the environment of the metal ions and, therefore, their chemical properties.

We have recently reported that a certain kind of compartmental Schiff base ligand can easily yield dinuclear complexes of the type $[M_2LL']$.[11] This kind of complex always shows two endogenous bridges and an additional exogenous link (L′) between the metal atoms, which influences the metal···metal separation, as well as the nuclearity of the complex. Thus, the $[M_2L]^+$ fragment can be used as a tecton that is susceptible of being extended through adequate connectors. In fact, this type of ligand can yield molecular zinc rectangles by using carbonate as the exogenous donor.[11a,d]

Among bridging ligands, carboxylates have been widely studied.[12–15] From these studies, it became apparent that mononuclear building blocks could be easily expanded through dicarboxylates, and it is well established that bridging coordination modes are encouraged through rigidity in the spacer of the ligand, which makes chelation geometrically impossible. However, no similar patterns have been described for carboxylate donors in polynuclear complexes generated from dinuclear nodes. In fact, the use of dinuclear tectons as precursors in the isolation of polynuclear complexes, especially those derived from compartmental ligands, is still poorly explored,[4–6] and, to the best of our knowledge, no relationships between the nature of the carboxylate and the nuclearity of this kind of complex have been reported to date. With these considerations in mind, we decided to investigate the influence of some carboxylate donors on the nuclearity of zinc complexes constructed from dinuclear cations. The photophysical properties of the complexes in solution and the solid state are also studied.

[a] *Departamento de Química Inorgánica, Facultade de Ciencias, Universidade de Santiago de Compostela, E-27002 Lugo, Spain. E-mail: qimatf69@usc.es*
[b] *Departamento de Química Inorgánica, Facultade de Química, Universidade de Santiago de Compostela, E-15706 Santiago de Compostela, Spain*
[c] *REQUIMTE, Faculdade de Ciências e Tecnologia, Universidade Nova de Lisboa, 2829-516 Monte de Caparica, Portugal*

† Electronic supplementary information (ESI) available: Space-filling diagrams for the molecular structures of **2–4**, ^{1}H NMR spectra comparison, mass spectrum for $[(Zn_2L^2)_2(OOC\text{–}CH_2\text{–}COO)]\cdot 6H_2O$, solution absorption and solid state emission spectra of ligands, and solution absorption, emission and excitation spectra of Zn(II) complexes with H_3L^1 and H_3L^2. See DOI: 10.1039/b710660b

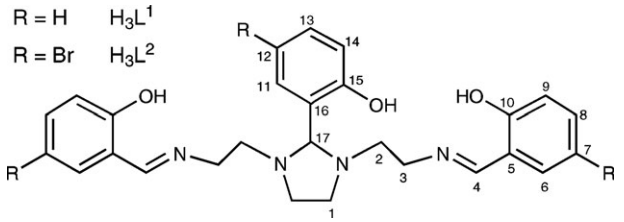

Scheme 1 Ligands used in this work, with the numbering scheme used for NMR studies.

Results and discussion

Synthesis

The carboxylate complexes were all prepared by mixing $Zn(acac)_2 \cdot H_2O$ with H_3L^x (x = 1, 2; Scheme 1) and the corresponding mono- or dicarboxylic acid under reflux in MeOH/MeCN (Scheme 2). The influence of the quantity of acid was investigated, meaning that 4 : 2 : 2 and 4 : 2 : 1 molar ratios of $Zn(acac)_2 \cdot H_2O$: H_3L^x : acid were tried. Nevertheless, the stoichiometry of the complexes obtained, as well as their purity and/or yield based on the amount of ligand used, seemed to be independent of the quantity of acid employed. In addition, the withdrawing bromine substituent on the phenol ring did not seem to have any effect on the nuclearity of the complexes. In this way, the reactions yielded dinuclear or tetranuclear complexes, according to the nature of the carboxylate ligand. Thus, on the one hand, *ortho*-phthalate and 4-formylbenzenecarboxylate lead to dinuclear complexes, while, on the other hand, malonate, succinate and terephthalate ligands were able to connect two $[Zn_2L^x]^+$ dinuclear blocks to yield tetranuclear compounds.

Therefore, the reaction of acetylacetonate salts with H_3L^x and carboxylic acids is a suitable synthetic route to obtain carboxylate complexes of compartmental ligands. Likewise, it represents an easy approach for systematically replacing the exogenous donor, though in this case, the nuclearity of the final product appears to be independent of the quantity of acid employed, while it clearly depends on the intrinsic characteristics of the carboxylate ligand.

All the complexes were fully characterised by elemental analysis, IR (Table 1), NMR, UV-vis and emission fluorescence spectroscopies, electrospray mass spectrometry and, in the case of $[Zn_2L^1(p\text{-}OOC\text{–}C_6H_4\text{–}CHO)] \cdot 2H_2O \cdot 2.5DMSO$ ($\mathbf{1} \cdot 2H_2O \cdot 2.5DMSO$), $[(Zn_2L^1)_2(OOC\text{–}CH_2CH_2\text{–}COO)] \cdot 4.25H_2O \cdot 0.75MeOH \cdot 0.5MeCN$ ($\mathbf{2} \cdot 4.25H_2O \cdot 0.75MeOH \cdot 0.5MeCN$), $[(Zn_2L^2)_2(OOC\text{–}CH_2CH_2\text{–}COO)] \cdot 7H_2O \cdot 0.25MeOH$ ($\mathbf{3} \cdot 7H_2O \cdot 0.25MeOH$) and $[Zn_2L^1(p\text{-}OOC\text{–}C_6H_4\text{–}COO)] \cdot 2.5H_2O \cdot MeOH \cdot 6EtOH$ ($\mathbf{4} \cdot 2.5H_2O \cdot MeOH \cdot 6EtOH$), by single crystal X-ray diffraction studies.

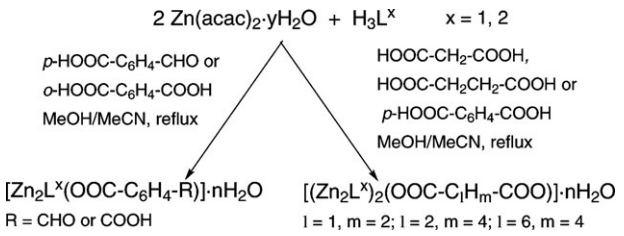

Scheme 2 Routes for the isolation of the metal complexes.

Single crystals of $\mathbf{1} \cdot 2H_2O \cdot 2.5DMSO$ and $\mathbf{4} \cdot 2.5H_2O \cdot MeOH \cdot 6EtOH$ were isolated by recrystallisation of the crude products shown in Table 1, whereas $\mathbf{2} \cdot 4.25H_2O \cdot 0.75MeOH \cdot 0.5MeCN$ and $\mathbf{3} \cdot 7H_2O \cdot 0.25MeOH$ were directly obtained from the reaction mixture. However, for these two compounds, all subsequent analyses demonstrated that they lost not only the volatile solvent molecules, but even water upon drying, yielding $\mathbf{2} \cdot 4.25H_2O$ and $\mathbf{3} \cdot 5H_2O$, respectively, as shown in Table 1.

Description of the crystal structures

Single crystals of $\mathbf{1} \cdot 2H_2O \cdot 2.5DMSO$, $\mathbf{2} \cdot 4.25H_2O \cdot 0.75MeOH \cdot 0.5MeCN$, $\mathbf{3} \cdot 7H_2O \cdot 0.25MeOH$ and $\mathbf{4} \cdot 2.5H_2O \cdot MeOH \cdot 6EtOH$, suitable for X-ray diffraction studies, were grown as detailed in the Experimental section.‡

$[Zn_2L^1(p\text{-}OOC\text{–}C_6H_4\text{–}CHO)] \cdot 2H_2O \cdot 2.5DMSO$ ($\mathbf{1} \cdot 2H_2O \cdot 2.5DMSO$). An ORTEP view of **1** is shown in Fig. 1. Experimental details are given in Table 2, and main distances and angles are listed in Table 3.

The asymmetric unit of $\mathbf{1} \cdot 2H_2O \cdot 2.5DMSO$ contains dinuclear neutral molecules of $[Zn_2L^1(p\text{-}OOC\text{–}C_6H_4\text{–}CHO)]$, with DMSO and water as solvates. In **1**, the heptadentate $(L^1)^{3-}$ Schiff base accommodates two zinc ions into its two N_2O compartments. Each one of them is formed by contiguous imine and imidazolidine N atoms, and a terminal phenol O atom, with the imidazolidine NCN group (N103–C120–N104) spanning both zinc ions. In addition, the central phenol O atom (O103) is bridging both metal atoms. The environments of the metal ions are completed by a 4-formylbenzenecarboxylate ligand, acting as a μ_2-η^1:η^1-*O*,*O* bridging donor in a *syn–syn* mode through the carboxylate group, with the aldehyde residue remaining uncoordinated. Accordingly, the zinc ions are triply-bridged by the endogenous NCN imidazolidine group and phenol O atom, and by the exogenous carboxylate ligand. This situation leads to N_2O_3 environments around the metal centres, with a separation of 3.2670(8) Å between them.

The τ parameter[16] (0.43 for Zn11 and 0.29 for Zn12) indicates a distorted square pyramidal environment for both zinc ions. The Zn–O and Zn–N distances, as well as the angles around the zinc atoms, agree with the proposed geometry, with the carboxylate O atoms at the apexes of the pyramids,[11a,d] while both pyramids share a basal vertex (O103). The Zn–O103 distances show the symmetry of the Zn–O_{phenol}–Zn bridge, with a Zn–O–Zn angle of *ca.* 110°.

$[(Zn_2L^1)_2(OOC\text{–}CH_2CH_2\text{–}COO)] \cdot 4.25H_2O \cdot 0.75MeOH \cdot 0.5MeCN$ ($\mathbf{2} \cdot 4.25H_2O \cdot 0.75MeOH \cdot 0.5MeCN$) and $[(Zn_2L_2)_2(OOC\text{–}CH_2CH_2\text{–}COO)] \cdot 7H_2O \cdot 0.25MeOH$ ($\mathbf{3} \cdot 7H_2O \cdot 0.25MeOH$). ORTEP views of **2** and **3** are shown in Fig. 2 and Fig. 3, respectively. Experimental details are given in Table 2, and the main distances and angles are listed in Table 4 and Table 5.

‡ For crystallographic data in CIF or other electronic format see DOI: 10.1039/b710660b

Table 1 Analytical and selected IR data for the complexes

Compound	N (%)[a]	C (%)[a]	H (%)[a]	ν(OH)[b]	ν(–C=N–)[b]
$[Zn_2L^1(OOC–C_6H_4–CHO)]\cdot 2H_2O$	7.43 (7.26)	54.15 (54.48)	4.36 (4.67)	3425	1629
$[Zn_2L^2(OOC–C_6H_4–CHO)]\cdot 2H_2O$	5.38 (5.55)	41.07 (41.62)	3.11 (3.27)	3454	1632
$[Zn_2L^1(o\text{-}OOC–C_6H_4–COOH)]\cdot 6H_2O$	6.33 (6.52)	48.88 (48.90)	4.73 (5.12)	3426	1633
$[Zn_2L^2(o\text{-}OOC–C_6H_4–COOH)]\cdot 3H_2O$	5.90 (5.38)	40.24 (40.32)	3.27 (3.26)	3404	1634
$[(Zn_2L^1)_2(OOC–CH_2–COO)]\cdot 10H_2O$	7.77 (7.70)	47.07 (47.05)	5.14 (5.23)	3429	1632
$[(Zn_2L^2)_2(OOC–CH_2–COO)]\cdot 6H_2O$	6.08 (6.04)	36.44 (36.87)	3.05 (3.34)	3403	1627
$[(Zn_2L^1)_2(OOC–CH_2CH_2–COO)]\cdot 4.25H_2O$	8.14 (8.21)	51.86 (51.02)	4.68 (4.87)	3438	1631
$[(Zn_2L^2)_2(OOC–CH_2CH_2–COO)]\cdot 5H_2O$	5.91 (6.05)	37.79 (37.60)	3.06 (3.35)	3440	1633
$[Zn_2L^1)_2(p\text{-}OOC–C_6H_4–COO)]\cdot 11H_2O$	7.06 (7.31)	48.43 (48.56)	5.09 (5.22)	3352	1628
$[(Zn_2L^2)_2(p\text{-}OOC–C_6H_4–COO)]\cdot 2H_2O$	6.07 (6.08)	40.10 (40.36)	2.99 (3.04)	3471	1633

[a] Found (calculated). [b] As KBr pellets; ν in cm^{-1}.

As the complexes are quite similar, they will be discussed together. The crystal structures of $\mathbf{2}\cdot 4.25H_2O\cdot 0.75MeOH\cdot 0.5MeCN$ and $\mathbf{3}\cdot 7H_2O\cdot 0.25MeOH$ are comprised of neutral molecules of $[(Zn_2L^x)_2(OOC–CH_2CH_2–COO)]$ (x = 1, 2), in addition to considerably disordered and dispersed molecules of methanol and water as solvates, and, in the case of **2**, acetonitrile as well. These two tetranuclear complexes can be understood as being self-assembled from two dinuclear $[Zn_2L^x]^+$ (x = 1, 2) nodes, joined by a bis-deprotonated succinate ligand.

The $[Zn_2L^x]^+$ sub-units, although not crystallographically equivalent, are closely akin, and, as occurred in **1**, both $(L^x)^{3-}$ ligands provide similar N_2O_2 donor sets to each Zn(II) ion. Two of these dinuclear sub-units are joined through a succinate ligand, acting as a μ_4-η^1:η^1:η^1:η^1 donor, with each carboxylate group coordinated in a *syn–syn* mode to both zinc atoms of one of the dinuclear nodes. Consequently, these Zn11···Zn12 and Zn21···Zn22 pairs show a triple bridge, very similar to that found in **1**.

As a result, the four zinc ions of each complex are also N_2O_3-coordinated, but in different distorted environments. In the case of **2**, the coordination geometries can be described as square pyramidal according to their τ values[16] (τ = 0.18 for Zn11, 0.40 for Zn12, 0.42 for Zn21 and 0.45 for Zn22), with carboxylate O atoms occupying the apexes of the pyramids. In contrast, the coordination environment of one of the zinc ions present in **3** (Zn11) should, according to its τ value of 0.67, be better described as distorted trigonal bipyramidal, while the others are lower than 0.5 (0.20 for Zn12, 0.44 for Zn21 and 0.40 for Zn22); consequently, they should be considered as square pyramids. Geometric data around the zinc centres are in agreement with highly distorted polyhedra, and do not merit further discussion as they are within their usual range for this type of Zn(II) complex.[11a,d]

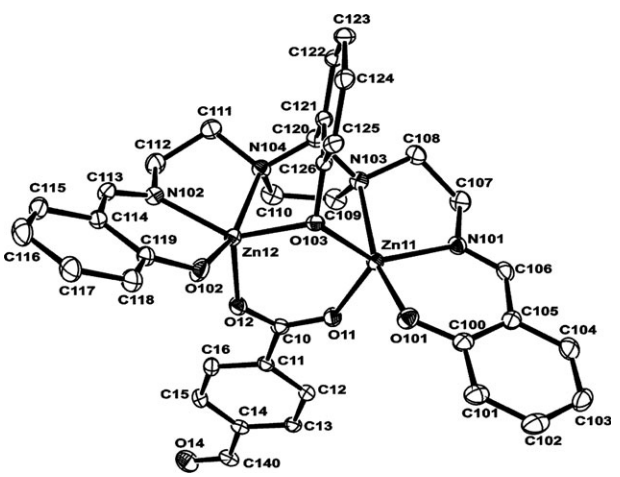

Fig. 1 Molecular structure of **1** showing the labelling scheme used. Ellipsoids are drawn at 50% probability.

In addition to this subtle disparity, these two complexes clearly display distinct intramolecular arrangements. Given the similitude not only between the dinuclear $[Zn_2L]^+$ tectons, but also concerning the coordination mode of the carboxylate groups, their disparity seems to depend on the conformation of the flexible ethylene spacers. These spacers, according to the torsion angles related to the succinate ligands (Table 4 and Table 5), are *gauche*-conformed in both cases. However, a significant difference can be observed for the carboxylate groups, which are almost parallel to the C11–C12 bond in the case of **2**, whereas for **3**, these COO^- groups are turned with respect to this central bond. As a result, although the Zn_2CO_3 metallacycles, formed by the phenolate and carboxylate bridges, are almost perpendicular in both compounds (Fig. 4), the intramolecular distances between O11···O21 and O12···O22 are *ca.* 4.37 Å in the case of **2**, whilst these are about 3.83 and 4.22 Å, respectively, for **3**. Likewise, this disparity leads to distances of *ca.* 7.30 and 7.63 Å for the respective Zn11···Zn21 and Zn12···Zn22 pairs present in **2**, while, correspondingly, these are about 6.63 and 7.09 Å for **3**.

Obviously, different intramolecular arrays involve different intramolecular interactions. Among them, it may be noteworthy to say that three weak π···π interactions can be considered for each complex, but **3** does not seem to display intramolecular C–H···π contacts, while up to three of them can be detected for **2**.

$[(Zn_2L^1)_2(p\text{-}OOC–C_6H_4–COO)]\cdot 2.5H_2O\cdot MeOH\cdot 6EtOH$ ($\mathbf{4}\cdot 2.5H_2O\cdot MeOH\cdot 6EtOH$). An ORTEP view of **4** is shown in Fig. 5. Experimental details are given in Table 2, and the main distances and angles are listed in Table 6.

The crystal structure of $\mathbf{4}\cdot 2.5H_2O\cdot MeOH\cdot 6EtOH$ resembles those of **2** and **3**, except for the rigidity of the carboxylate ligand and the crystallographic symmetry. Thus, the crystal structure is comprised of neutral tetranuclear $[(Zn_2L^1)_2(p\text{-}OOC–C_6H_4–COO)]$ molecules, in addition to ethanol, methanol and water molecules as solvates. As also occurs in

Table 2 Crystal data and structure refinement for **1** · $2H_2O$ · 2.5DMSO to **4** · $2.5H_2O$ · MeOH · 6EtOH

	1 · $2H_2O$ · 2.5DMSO	**2** · $4.25H_2O$ · 0.75MeOH · 0.5MeCN	**3** · $7H_2O$ · 0.25MeOH	**4** · $2.5H_2O$ · MeOH · 6EtOH
Empirical formula	$C_{40}H_{49}N_4O_{9.5}S_{2.5}Zn_2$	$C_{59.75}H_{68}N_{8.5}O_{15}Zn_4$	$C_{58.25}H_{61.5}N_8O_{17.25}Br_6Zn_4$	$C_{75}H_{103}N_8O_{19.5}Zn_4$
Formula weight	948.72	1406.71	1850.59	1682.13
Crystal size/mm	0.43 × 0.41 × 0.23	0.20 × 0.15 × 0.07	0.37 × 0.27 × 0.01	0.53 × 0.44 × 0.18
Crystal system	Monoclinic	Monoclinic	Monoclinic	Triclinic
Space group	$P2_1/n$ (no. 14)	$P2_1/c$ (no. 14)	$P2_1/c$ (no. 14)	P-1 (no. 2)
a/Å	15.004(2)	16.690(1)	19.312(1)	10.184(2)
b/Å	14.696(2)	18.584(1)	22.964(1)	11.268(3)
c/Å	20.069(3)	23.409(1)	17.884(1)	19.979(5)
α/°	90	90	90	92.722(4)
β/°	106.691(3)	97.59(1)	106.23(2)	104.558(4)
γ/°	90	90	90	111.284(4)
V/Å^3	4238.6(11)	7197.5(3)	7615.0(7)	2043.1(9)
Z	4	4	4	1
Absorption coefficient/mm^{-1}	1.314	1.380	4.458	1.231
Reflections collected	35 811	72 041	74 944	35 795
Independent reflections	8693 [R_{int} = 0.0305]	12 804 [R_{int} = 0.0666]	13 562 [R_{int} = 0.0709]	7165 [R_{int} = 0.0358]
Data/restraints/parameters	8693/0/559	12 804/0/823	13 562/0/865	7165/0/477
Final R indices [$I > 2\sigma(I)$]	R_1 = 0.0460; wR_2 = 0.1128	R_1 = 0.0770; wR_2 = 0.2300	R_1 = 0.0590; wR_2 = 0.1432	R_1 = 0.0465; wR_2 = 0.1411
R indices (all data)	R_1 = 0.0802; wR_2 = 0.1351	R_1 = 0.1154; wR_2 = 0.2555	R_1 = 0.1147; wR_2 = 0.1622	R_1 = 0.0594; wR_2 = 0.1502
CCDC number	299594	660829	660830	299595

2 and **3**, **4** can be understood as being self-assembled from two dinuclear $[Zn_2L^1]^+$ nodes joined by a dicarboxylate ligand, *i.e.* terephthalate in this case. **4** shows an inversion centre, located on the centroid of the aromatic ring of the dicarboxylate donor ($' = 2 - x, 1 - y, -z$). Accordingly, both $[Zn_2L^1]^+$ cations are crystallographically equivalent, and their arrangements are similar to those described for **1–3**. Both zinc ions are N_2O_2-tetracoordinated, with the Schiff base providing an NCN and a phenol O bridge between the metal atoms.

As also occurred in **2** and **3**, two dinuclear cations are joined by an exogenous terephthalate ligand, again acting in a μ_4-η^1:η^1:η^1:η^1 fashion, which completes the coordination spheres of the zinc centres. Therefore, each Zn11···Zn12 pair is also triply-bridged, giving rise to a Zn···Zn separation of 3.2003(10) Å within the $[Zn_2L^1]^+$ unit, with a Zn–O103–Zn angle of *ca.* 107°. Accordingly, in this case, the complex is a molecular rectangle, with sides of *ca.* 3 and 11 Å. The four zinc ions at the vertexes of the rectangle are, once again, N_2O_3 coordinated, with τ parameters close to 0.45 (τ = 0.45 for Zn11 and 0.44 for Zn12). These values again indicate that the square pyramidal environment of the zinc centres is highly distorted, with the carboxylate O atoms at the apexes of the pyramids.

Table 3 Main distances (/Å) and angles (/°) for **1** · $2H_2O$ · 2.5DMSO

Zn11–O101	1.980(3)	Zn12–O102	1.981(3)
Zn11–N101	2.036(3)	Zn12–N102	2.032(3)
Zn11–N103	2.338(3)	Zn12–N104	2.381(3)
Zn11–O103	1.995(3)	Zn12–O103	1.995(3)
Zn11–O11	1.999(3)	Zn12–O12	1.972(3)
Zn11···Zn12	3.2670(8)		
O11–Zn11–O101	99.87(12)	O12–Zn12–O102	105.07(12)
O11–Zn11–N101	111.89(12)	O12–Zn12–N102	108.10(13)
O11–Zn11–N103	96.09(12)	O12–Zn12–N104	95.78(12)
O11–Zn11–O103	108.09(11)	O12–Zn12–O103	108.25(11)
O103–Zn11–N101	138.07(12)	O103–Zn12–N102	141.56(12)
O101–Zn11–N103	163.43(12)	O102–Zn12–N104	158.72(12)
Zn11–O103–Zn12	109.94(12)		

Due to the rigidity of the terephthalate ligand, the distance between the Zn11···Zn12′ and Zn11′···Zn12 pairs (10.694(3) Å) is longer than for **2** and **3**. Besides, the different flexibilities of the spacers in **2–4** leads to dissimilar intramolecular arrangements for these three tetranuclear complexes (Fig. S1 of ESI†).

IR spectroscopy

The IR spectra of all the complexes show an intense band in the range 1627–1634 cm^{-1} (Table 1), in accordance with the coordination of the Schiff base to the metal atoms through the imine N atoms. Besides, a broad band centred at *ca.* 3400 cm^{-1} is consistent with the hydration of all the metal complexes.

NMR spectroscopy

The ^{1}H NMR spectra of all the complexes were recorded using DMSO-d_6 as the solvent. The spectra show two sets of aromatic signals: one for the two terminal ligand arms,

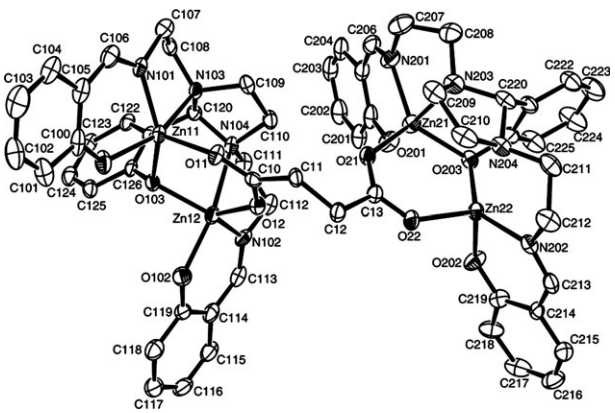

Fig. 2 ORTEP diagram of **2** showing the labelling scheme used. Ellipsoids are drawn at 40% probability.

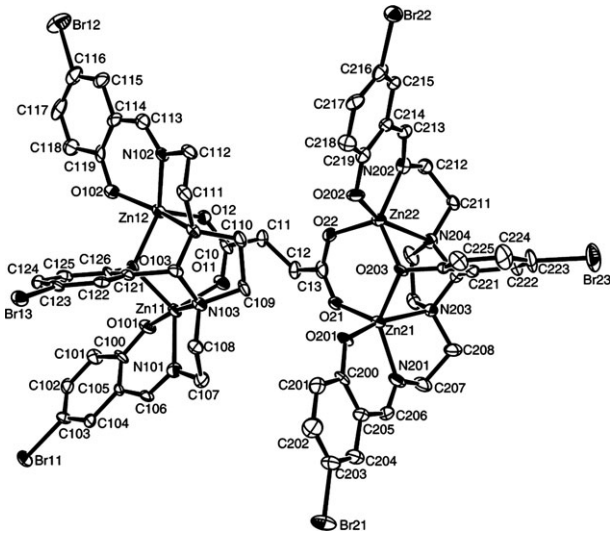

Fig. 3 ORTEP diagram of **3** showing the labelling scheme used. Ellipsoids are drawn at 50% probability.

indicating that they are magnetically equivalent, and the other for the middle arm. All of the signals could be fully assigned from COSY experiments and by comparison with previous results.[11a,d,17] The high resolution of the spectra are consistent with the high purity of the isolated compounds, indicating that they are unique in solution.

The main conclusions from this study concern the nuclearity of the complexes. Thus, the complexes obtained from aromatic carboxylates show some new signals in the aromatic region, in addition to those corresponding to the free ligand (Fig. S2 of ESI†). Accordingly, $[Zn_2L^x(p\text{-}OOC\text{–}C_6H_4\text{–}CHO)]$ and $[Zn_2L^x(o\text{-}OOC\text{–}C_6H_4\text{–}COOH)]$ present two new doublets (2H each) at *ca.* 8.0 and 7.5 ppm, respectively, and $[(Zn_2L^x)_2(p\text{-}OOC\text{–}C_6H_4\text{–}COO)]$ shows a new singlet (4H) at *ca.* 7.9 ppm, in agreement with the coordination of the carboxylate ligand to the metal atoms. Moreover, the relative intensity of the imine and carboxylate aromatic hydrogen atoms clearly demonstrates the 1 : 1 Schiff base ligand : carboxylate ratio for $[Zn_2L^x(p\text{-}OOC\text{–}C_6H_4\text{–}CHO)]$ and $[Zn_2L^x(o\text{-}OOC\text{–}C_6H_4\text{–}COOH)]$, and the 2 : 1 Schiff base ligand : terephthalate ratio for $[(Zn_2L^x)_2(p\text{-}OOC\text{–}C_6H_4\text{–}COO)]$, in accordance with the proposed formulation.

In the case of the complexes obtained from aliphatic carboxylates, $[(Zn_2L^x)_2(OOC\text{–}CH_2\text{–}COO)]$ and $[(Zn_2L^x)_2(p\text{-}OOC\text{–}CH_2CH_2\text{–}COO)]$, the ^{1}H NMR spectra do not allow the establishment of the Schiff base : carboxylate ratio in all cases. Thus, the ^{1}H NMR spectra of $[(Zn_2L^x)_2(OOC\text{–}CH_2CH_2\text{–}COO)]$ show a new singlet at *ca.* 2.48 ppm (4H) in a 1 : 1 molar ratio with the imine hydrogen atoms. This, therefore, suggests a tetranuclear nature in these complexes in solution, in agreement with solid state results. However, in the case of malonate complexes, due to the high number of aliphatic protons and solvent signals in the region 2–4 ppm, those signals corresponding to the $–CH_2–$ moieties of the carboxylate donor (which should appear about 3 ppm) could not be unequivocally assigned. Therefore, the stoichiometry of the complexes could not be inferred. Nevertheless, the presence of the malonate ligand, as well as the succinate ligand, is supported by ^{13}C NMR spectroscopy: two new signals are observed at *ca.* 46 and 175 ppm for the malonate complexes, and at *ca.* 32 and 180 ppm for the succinate compounds, and can be assigned to the aliphatic and carbonyl carbon atoms of the carboxylate ligands, respectively. Thus, NMR spectroscopy also substantiates the isolation of malonate and succinate complexes in high purity, although it does not allow the $[Zn_2L^x]^+$: malonate ratio to be determined.

Table 4 Selected distances (/Å) and angles (/°) for **2**·4.25H_2O·0.75MeOH·0.5MeCN

Zn11–O11	1.970(4)	Zn21–O21	1.980(5)
Zn11–O103	1.970(4)	Zn21–O203	1.991(5)
Zn11–O101	1.990(5)	Zn21–N201	2.008(6)
Zn11–N101	2.017(5)	Zn21–O201	2.012(5)
Zn11–N103	2.287(6)	Zn21–N203	2.378(6)
Zn12–O103	1.987(4)	Zn22–O203	1.960(5)
Zn12–O12	1.989(5)	Zn22–O22	1.977(5)
Zn12–O102	1.993(5)	Zn22–O202	1.985(5)
Zn12–N102	1.997(6)	Zn22–N202	2.000(5)
Zn12–N104	2.403(6)	Zn22–N204	2.459(5)
Zn11···Zn12	3.2634(11)	Zn21···Zn22	3.2443(10)
Zn11···Zn21	7.2987(13)	Zn12···Zn22	7.6294(12)
O11–Zn11–O103	104.64(19)	O21–Zn21–O203	111.87(18)
O11–Zn11–O101	102.3(2)	O21–Zn21–O201	104.3(2)
O11–Zn11–N101	107.8(2)	O21–Zn21–N201	109.4(2)
O11–Zn11–N103	99.83(19)	O21–Zn21–N203	93.3(2)
O101–Zn11–N103	157.6(2)	O201–Zn21–N203	162.0(2)
O103–Zn11–N101	146.5(2)	O203–Zn21–N201	136.8(2)
O12–Zn12–O103	109.69(19)	O22–Zn22–O203	105.80(19)
O12–Zn12–O102	104.6(2)	O22–Zn22–O202	100.4(2)
O12–Zn12–N102	111.6(2)	O22–Zn22–N202	113.6(2)
O12–Zn12–N104	94.98(19)	O22–Zn22–N204	94.9(2)
O102–Zn12–N104	160.4(2)	O202–Zn22–N204	164.5(2)
O103–Zn12–N102	136.1(2)	O203–Zn22–N202	137.4(2)
Zn11–O103–Zn12	111.1(2)	Zn22–O203–Zn21	110.4(2)
O11–C10–C11–C12	173.3(6)	C11–C12–C13–O21	−8.8(10)
O12–C10–C11–C12	−6.2(9)	C11–C12–C13O22	170.6(6)
C10–C11–C12 C13	86.8(8)		

Table 5 Selected distances (/Å) and angles (/°) for **3**·7H_2O·0.25MeOH

Zn11–O11	1.976(5)	Zn21–O21	1.988(6)
Zn11–O103	1.988(5)	Zn21–O203	1.971(5)
Zn11–O101	2.011(6)	Zn21–O201	1.997(5)
Zn11–N101	2.017(7)	Zn21–N201	2.013(7)
Zn11–N103	2.320(6)	Zn21–N203	2.397(7)
Zn12–O12	1.976(5)	Zn22–O22	1.979(6)
Zn12–O103	2.004(5)	Zn22–O203	1.971(5)
Zn12–O102	2.006(6)	Zn22–O202	1.981(5)
Zn12–N102	2.036(6)	Zn22–N202	2.020(7)
Zn12–N104	2.370(7)	Zn22–N204	2.494(6)
Zn11···Zn12	3.2730(13)	Zn21···Zn22	3.2704(12)
Zn11···Zn21	6.6271(14)	Zn12···Zn22	7.0891(14)
O11–Zn11–O103	107.5(2)	O21–Zn21–O203	106.1(2)
O11–Zn11–O101	97.0(2)	O21–Zn21–O201	104.5(2)
O11–Zn11–N101	125.2(2)	O21–Zn21–N201	111.7(3)
O11–Zn11–N103	95.3(2)	O21–Zn21–N203	90.5(2)
O101–Zn11–N103	166.5(2)	O201–Zn21–N203	164.8(2)
O103–Zn11–N101	126.1(2)	O203–Zn21–N201	138.4(3)
O12–Zn12–O103	104.9(2)	O22–Zn22–O203	109.8(2)
O12–Zn12–O102	104.1(2)	O22–Zn22–O202	104.2(2)
O12–Zn12–N102	111.0(2)	O22–Zn22–N202	111.7(2)
O12–Zn12–N104	101.2(2)	O22–Zn22–N204	96.8(2)
O102–Zn12–N104	154.7(2)	O202–Zn22–N204	158.9(2)
O103–Zn12–N102	142.9(2)	O203–Zn22–N202	135.0(2)
Zn11–O103–Zn12	110.1(2)	Zn21–O203–Zn22	112.1(3)
O12–C10–C11–C12	161.1(7)	C11–C12–C13–O21	147.9(7)
O11–C10–C11–C12	−19.9(10)	C11–C12–C13–O22	−34.0(10)
C10–C11–C12–C13	−75.2(9)		

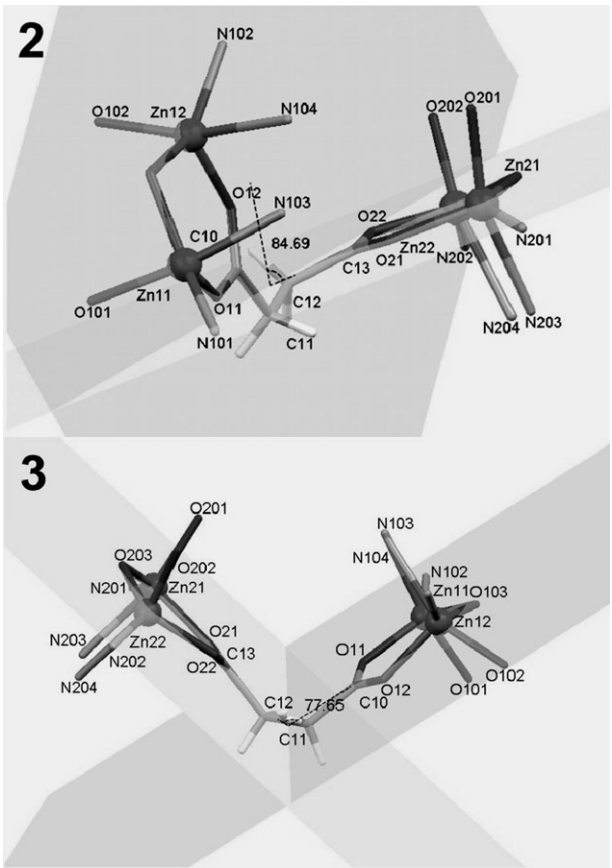

Fig. 4 Zn(II) coordination environments for **2** and **3**, joined by the succinate ligands, showing the angle between the calculated planes corresponding to the metallacycles formed by the phenolate and carboxylate bridges, and their distortions.

Mass spectrometry

Electrospray mass spectra of methanol solutions of all the complexes showed an intense peak due to $[Zn_2L^x]^+$ fragments, in agreement with the presence of the basic dinuclear node in solution. Besides this, it was possible to observe the molecular peaks for all the complexes. Thus, electrospray mass spectra indicated that $[Zn_2L^x(p\text{-}OOC\text{–}C_6H_4\text{–}CHO)]$ and $[Zn_2L^x(o\text{-}OOC\text{–}C_6H_4\text{–}COOH)]$ are dinuclear in solution, with peaks related to the $[M + H]^+$ or $[M + Na]^+$ fragments. No peaks associated with higher nuclearity fragments were detected in these cases. However, the complexes derived from terephthalic, malonic and succinic acids presented peaks of high intensity due to $[(Zn_2L^x)_2(OOC\text{–}C_lH_m\text{–}COOH)]^+$ or $[(Zn_2L^x)_2(OOC\text{–}C_lH_m\text{–}COO)Na]^+$ fragments ($l = 1$, $m = 2$; $l = 2$, $m = 4$; $l = 6$, $m = 4$), in agreement with their tetranuclear nature in solution (Fig. S3 of ESI†). No other peaks of higher m/z were detected for the tetranuclear complexes.

As a result of this study, it can be inferred that the complexes seem to retain their dinuclear or tetranuclear character, with the external ligands coordinated to the metal ions in solution. Besides this, although the ^{1}H NMR spectra do not allow the nuclearity of the malonate complexes to be determined, their mass spectrometry clearly shows that they retain a tetranuclear nature in solution.

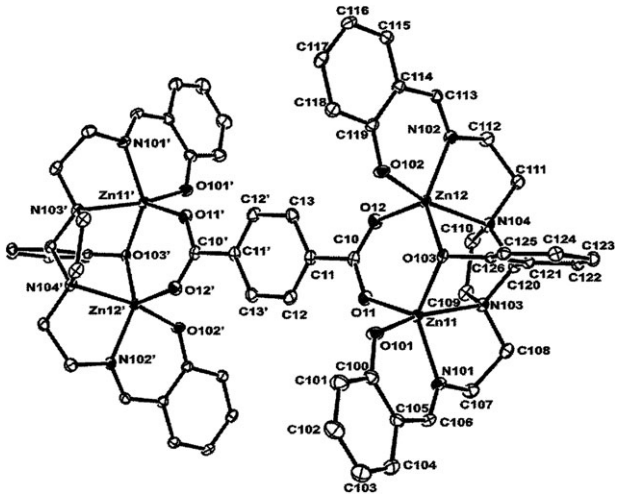

Fig. 5 Molecular structure of **4** showing the labelling scheme used. Symmetry code $' = 2 - x, 1 - y, -z$. Ellipsoids are drawn at 30% probability.

Therefore, this study seems to indicate that flexible dicarboxylate ligands bridge dinuclear nodes to yield tetranuclear complexes, while the nuclearity of benzene-based carboxylate complexes strongly depends on the relative position of the carboxylic functions. Thus, *ortho*-phthalate can only give rise to dinuclear complexes, maybe due to steric hindrance caused by the folding of the Schiff base ligands, so preventing the growth of the initial blocks. However, this effect is avoided by the use of terephthalate, which maintains the dinuclear blocks far enough apart. Furthermore, the complexes of this rigid linker can be defined as molecular rectangles, which do not occur with the succinate flexible bridge. Likewise, 4-formylbenzenecarboxylate also gives rise to dinuclear complexes, with the formyl group remaining uncoordinated.

Hence, these results suggest that it is easy to achieve tetranuclearity by using this kind of $[Zn_2L^x]^+$ node, but not coordination polymers. This is in agreement with the most general pattern found in the literature for the dinuclear tectons of dinucleating ligands,[5] although a small number of coordination polymers have been grown from this kind of tecton and dicarboxylates.[6a,c] In our case, this could be related to the wrapping character of the Schiff base, which only makes the metal ion accessible from one side of the $[Zn_2L^x]^+$ node

Table 6 Selected distances (/Å) and angles (/°) for $4 \cdot 2.5H_2O \cdot MeOH \cdot 6EtOH$[a]

Zn11–O101	1.990(3)	Zn12–O102	1.986(3)
Zn11–N101	2.001(3)	Zn12–N102	2.012(3)
Zn11–N103	2.382(3)	Zn12–N104	2.296(3)
Zn11–O103	1.993(3)	Zn12–O103	1.992(2)
Zn11–O11	1.978(3)	Zn12–O12	1.968(3)
Zn11···Zn12	3.2003(10)	Zn11···Zn12′	10.694(3)
O11–Zn11–O101	98.28(12)	O12–Zn12–O102	97.45(12)
O11–Zn11–O103	109.66(11)	O12–Zn12–O103	110.97(11)
O11–Zn11–N101	113.16(13)	O12–Zn12–N102	109.57(13)
O11–Zn11–N103	98.51(11)	O12–Zn12–N104	96.93(12)
O101–Zn11–N103	163.07(11)	O102–Zn12–N104	165.22(12)
O103–Zn11–N101	135.87(12)	O103–Zn12–N102	138.73(12)
Zn12–O103–Zn11	106.87(11)		

[a] Symmetry code $' = 2 - x, 1 - y, -z$.

Table 7 UV/vis and fluorescence data for ligands H_3L^1 and H_3L^2 and their Zn(II) complexes in solution

Compound	UV/vis λ_{max}/nm	Fluorescence λ_{em}/nm	Φ_F	Stokes' shift/nm	Solvent
H_3L^1	257, 315, 404	No emission	—	—	EtOH
					DMSO
H_3L^2	255 (sh),[a] 332, 417	No emission	—	—	EtOH
					DMSO
$[Zn_2L^1(OOC–C_6H_4–CHO)]\cdot 2H_2O$	370	450	0.29	80	EtOH
	370	449	0.20	79	DMSO
$[Zn_2L^2(OOC–C_6H_4–CHO)]\cdot 2H_2O$	382	455	0.09	73	EtOH
$[Zn_2L^1(o\text{-}OOC–C_6H_4–COOH)]\cdot 6H_2O$	370	445	0.31	75	DMSO/EtOH
$[Zn_2L^2(o\text{-}OOC–C_6H_4–COOH)]\cdot 3H_2O$	380	455	0.13	75	EtOH
$[(Zn_2L^1)_2(OOC–CH_2–COO)]\cdot 10H_2O$	370	450	0.38	80	EtOH
$[(Zn_2L^2)_2(OOC–CH_2–COO)]\cdot 6H_2O$	381	452	0.15	71	DMSO
$[(Zn_2L^1)_2(OOC–CH_2CH_2–COO)]\cdot 4H_2O$	375	455	0.54	80	DMSO
$[(Zn_2L^2)_2(OOC–CH_2CH_2–COO)]\cdot 5H_2O$	382	455	0.16	80	DMSO
$[(Zn_2L^1)_2(p\text{-}OOC–C_6H_4–COO)]\cdot 11H_2O$	370	446	0.18	76	DMSO/EtOH
$[(Zn_2L^2)_2(p\text{-}OOC–C_6H_4–COO)]\cdot 2H_2O$	382	455	0.14	73	DMSO

[a] (sh) = shoulder.

(Fig. S1 of ESI†). Accordingly, it appears that the role of carboxylates as the connectors of dinuclear tectons of compartmental ligands is greatly influenced by the intrinsic characteristics of the compartmental donor *per se*, and that the relationship between the carboxylate and nuclearity is not as simple as in the complexes constructed from mononuclear blocks.

Photophysical study

The spectral and photophysical parameters (wavelength maxima of absorption and emission spectra, and fluorescence quantum yields (ϕ_F)) of the free ligands, and all of the carboxylate complexes in absolute ethanol or DMSO/EtOH solutions at 298 K, are summarised in Table 7.

The photophysical properties of the free Schiff base ligands were analysed in order to compare them with those of their corresponding zinc complexes and to test their ability to recognize Zn(II) in solution. Thus, the solution absorption spectra of H_3L^1 and H_3L^2 were recorded (Fig. S4 of ESI†), and in both cases showed three bands (Table 7) that could be attributed to π–π* electronic transitions of the phenol rings and the imine bonds present in both molecules.[18] These results are in accordance with those previously reported for H_3L^1 by Orvig *et al.*[17] However, the 400 nm excitation of DMSO or absolute ethanol solutions of the ligands showed no emission. This could be ascribed to the existence of hydrogen bond interactions between the ligands and the polar solvents in solution, so increasing the non-radioactive pathways in both molecules.[19] Nevertheless, both ligands are fluorescent in the solid state, with the spectra showing a broad and intense band centred at 530 nm (normalised emission spectra in solid state reported in Fig. S4B of the ESI†).

The chemosensor abilities of H_3L^1 and H_3L^2 towards Zn(II) in absolute ethanol solution were also studied, and the absorption spectra of mixtures of Zn(II) salts and ligands in 1 : 1 and 2 : 1 molar ratios were recorded. The bands of these spectra showed a red-shift with respect to the free ligand, centred at 315 nm (H_3L^1) and 332 nm (H_3L^2), after the addition of one

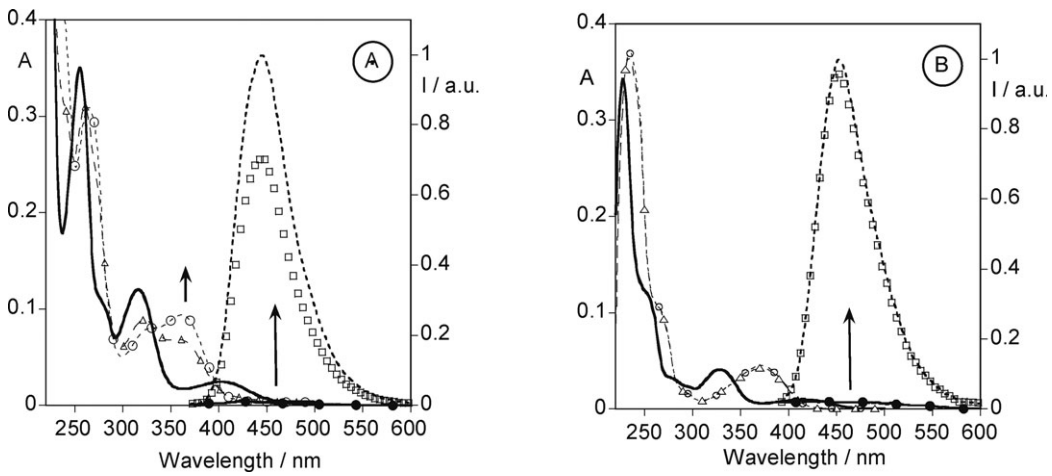

Fig. 6 (A) Absorption (— H_3L^1, –△– H_3L^1Zn(II), ···○··· $H_3L^1Zn_2$) and emission (–●– H_3L^1, □ H_3L^1Zn, ··· $H_3L^1Zn_2$) spectra for free H_3L^1, and in the presence of one and two equivalents of Zn(II) ($[H_3L^1] = 10^{-5}$ M; λ_{exc} = 315 and 404 nm). (B) Absorption (— H_3L^2, –△– H_3L^2Zn(II), ···○··· $H_3L^2Zn_2$) and emission (–●– H_3L^2, □ H_3L^2Zn, ··· $H_3L^2Zn_2$) spectra for free H_3L^2, and in the presence of one and two equivalents of Zn(II) ($[H_3L^2] = 10^{-5}$ M; λ_{exc} = 332 nm).

Table 8 Fluorescence emission of Zn(II) complexes in the solid state[a]

Compound	λ_{em}/nm	Intensity[a]	Colour
$[Zn_2L^1(OOC–C_6H_4–CHO)]\cdot 2H_2O$	453, 548	Very low	Greenish
$[Zn_2L^2(OOC–C_6H_4–CHO)]\cdot 2H_2O$	550	Very low	Green
$[Zn_2L^1(o\text{-}OOC–C_6H_4–COOH)]\cdot 6H_2O$	487	High	Bluish
$[Zn_2L^2(o\text{-}OOC–C_6H_4–COOH)]\cdot 3H_2O$	465	High	Bluish
$[(Zn_2L^1)_2(OOC–CH_2–COO)]\cdot 10H_2O$	450	High	Blue
$[(Zn_2L^2)_2(OOC–CH_2–COO)]\cdot 6H_2O$	471	High	Bluish
$[(Zn_2L^1)_2(OOC–CH_2CH_2–COO)]\cdot 4H_2O$	471	High	Bluish
$[(Zn_2L^2)_2(OOC–CH_2CH_2–COO)]\cdot 5H_2O$	478	Low	Bluish
$[(Zn_2L^1)_2(p\text{-}OOC–C_6H_4–COO)]\cdot 11H_2O$	469	Low	Bluish
$[(Zn_2L^2)_2(p\text{-}OOC–C_6H_4–COO)]\cdot 2H_2O$	590	High	Yellowish

[a] The relative intensity is always compared with complexes of the same ligand.

and two equivalents of the metal ion. This shift is commonly observed upon metal complexation. Besides this, excitation of the solutions at 315 and 404 nm [Zn(II) + H_3L^1], and at 332 nm [Zn(II) + H_3L^2], produced a strong fluorescence emission in both cases, centred at 455 and 450 nm for H_3L^1- and H_3L^2-containing solutions, respectively (Fig. 6). These results show the strong ability of this kind of ligand to recognize Zn(II) ions in solution.

The absorption, emission and excitation spectra of all the complexes in absolute ethanol or DMSO/absolute ethanol mixtures at 298 K were recorded, and are reported in Figs. S5 and S6 of the ESI.† In all cases, the solution fluorescence spectra appear to be mirror-symmetrical with the long-wavelength band of the corresponding absorption spectra, assuming the position of the absorption and emission bands are not dependent on solvent polarity.

In addition, these analyses show that all of the synthesised Zn(II) complexes are emissive in solution, with moderate to high fluorescence quantum yields (Table 7). The most emissive complexes are $[(Zn_2L^1)_2(OOC–CH_2CH_2–COO)]\cdot 4H_2O$ (Φ_F = 0.54), $[(Zn_2L^1)_2(OOC–CH_2–COO)]\cdot 10H_2O$ (Φ_F = 0.38), $[Zn_2L^1(o\text{-}OOC–C_6H_4–COOH)]\cdot 6H_2O$ (Φ_F = 0.31) and $[Zn_2L^1(OOC–C_6H_4–CHO)]\cdot 2H_2O$ (Φ_F = 0.29). Since all of them contain H_3L^1, this result suggests that the bromine atom present in H_3L^2 partially quenches the emission by the halide atom effect.[20]

The fluorescence properties of the complexes have also been studied in the solid state (Table 8, Fig. 7). All of the yellow solids seem emissive, and, therefore, steady-state fluorescence emission measurements at room temperature were recorded by using an optical fiber device connected to the spectrofluorimeter. It should be noted that the emission band in the solid state spectra (Fig. 7) are broader than those observed in solution.

These solid state studies allow an emission pattern to be drawn as being a function of the aromatic ring substituent and carboxylate donor present in the complex. Thus, 4-formylbenzenecarboxylate produces the least emissive solid complexes (Table 8), both with green and greenish emissions. For the remaining carboxylate complexes, a general pattern cannot be deduced, although the most emissive complexes contain an aliphatic carboxylate, both with H_3L^1 and H_3L^2. Likewise, complexes with identical carboxylate groups generally show a stronger red-shift when they contain $[L^2]^{3-}$. In this way, a strong red-shift is observed in $[(Zn_2L^2)_2(p\text{-}OOC–C_6H_4–COO)]\cdot 2H_2O$, where the terephthalate anion is coordinated, giving a yellow emissive compound. Malonate, succinate and *ortho*-phthalate complexes show various blue and green light emissions (Table 8, Fig. 7).

Therefore, we have observed that the colour of the emitted light can be modulated by complexation of different carboxylate donors to Zn(II) metal ions, and by the presence of aromatic ring substituents on the Schiff base. Thus, the solid state fluorescence emission observed for the metal complexes could represent a very attractive alternative to the usual inorganic hybrid materials used as the active layer in light-emitting diode devices (LEDs) and lasers. In fact, during the last few years, many Zn(II) complexes have been reported in the literature as being suitable compounds for new LEDs.[21] The changes in luminescence observed at room temperature for the complexes described herein could be an interesting property in order to explore their use in material science.

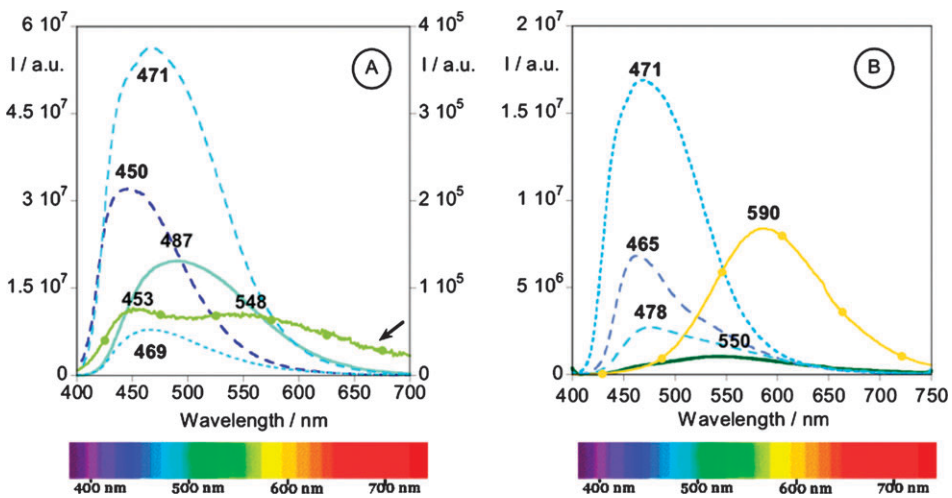

Fig. 7 Emission spectra in solid state at 298 K for: (A) Zn(II) complexes of H_3L^1 (λ_{exc} = 370 nm) and (B) Zn(II) complexes of H_3L^2 (λ_{exc} = 380 nm).

Conclusions

Dinuclear and tetranuclear carboxylate complexes of two dinucleating Schiff bases can be easily isolated by direct interaction between zinc acetylacetonate, the Schiff base and the corresponding carboxylic acid. The nuclearity of the complexes seem to depend on the flexibility of the backbone spacer and on the relative positions of the carbonyl moieties in the carboxylate ligand.

Accordingly, flexible dicarboxylates, such as malonate and succinate, bridge dinuclear $[Zn_2L^x]^+$ nodes to yield tetranuclear complexes, while the nuclearity of benzene-based carboxylate complexes strongly depends on the relative position of the carboxylic functions. In this way, *ortho*-phthalate precludes the growth of the initial blocks, probably due to steric hindrance caused by the folding of the Schiff base ligand. This effect is avoided by the use of terephthalate, which keeps the dinuclear nodes apart. Furthermore, the complexes of this rigid linker can be defined as molecular rectangles, while the succinate compounds do not form a regular polygon, showing that the flexibility of the carbon backbone plays an important role in the shape of the molecular polyhedra. In addition, 4-formylbenzenecarboxylate also gives rise to dinuclear complexes, illustrating the inability of the formyl group to act as a donor in this type of complex.

Besides this, it is apparent that this kind of compartmental dicarboxylate ligand could yield molecular rectangles with sides of predicted length, or tetranuclear complexes, but could not give rise to molecular polymers. Finally, the complexes are luminescent, both in solution and in solid state, which could be of significance in the search for new LEDs.

Experimental

General remarks

Elemental analyses of C, H and N were performed on a Carlo Erba EA 1108 analyzer. NMR spectra were recorded on a Bruker AC-300 spectrometer using DMSO-d_6 as the solvent. Infrared spectra were recorded as KBr pellets on a Bio-Rad FTS 135 spectrophotometer in the range 4000–600 cm^{-1}. Electrospray mass spectra were obtained on a Hewlett-Packard LC/MS spectrometer with methanol as the solvent.

Synthesis

H_3L^x (x = 1, 2) were synthesized by following a method previously described and were satisfactorily characterized.[11,17] All solvents, $Zn(acac)_2 \cdot yH_2O$, and *ortho*-phthalic, terephthalic, malonic, succinic and 4-formylbenzenecarboxylic acids are commercially available and were used without further purification.

All the carboxylate complexes of $Zn_2L^x(OOC–C_6H_4–R)$ stoichiometry (R = CHO or COOH) were obtained in a similar way, which is exemplified by the isolation of $[Zn_2L^1(OOC–C_6H_4–CHO)] \cdot 2H_2O \cdot 2.5DMSO$ ($\mathbf{1} \cdot 2H_2O \cdot 2.5DMSO$).

$[Zn_2L^1(OOC–C_6H_4–CHO)] \cdot 2H_2O \cdot 2.5DMSO$ ($\mathbf{1} \cdot 2H_2O \cdot 2.5DMSO$). To a methanol solution (60 mL) of zinc acetylacetonate hydrate (0.54 g, 2.04 mmol) in a 100 mL round-bottomed flask were added H_3L^1 (0.46 g, 1.02 mmol) and acetonitrile (20 mL). The mixture was stirred until a yellow solution was obtained. Next, 4-formylbenzenecarboxylic acid (0.15 g, 1.02 mmol) was added and the flask equipped with a water-cooled condenser. The mixture was heated to reflux with stirring for 4 h, and the yellow solid that precipitated was filtered off and dried in air. Its elemental analysis was in agreement with the stoichiometry $[Zn_2L^1(OOC–C_6H_4–CHO)] \cdot 2H_2O$ ($\mathbf{1} \cdot 2H_2O$). Yield: 0.51 g (65%), mp >300 °C. MS (ES): m/z 587.2 ($[Zn_2L^1]^+$), 759.0 ($[Zn_2L^1(OOC–C_6H_4–CHO)Na]^+$). ^{1}H NMR (300 MHz, DMSO-d_6): δ 2.79–2.62 (m, 6H), 3.39–3.31 (m, 2H), 3.52 (d, 2H), 3.77 (t, 2H) (H1 + H2 + H3); 4.14 (s, 1H, H17); 6.39 (t, 2H, H7); 6.80–6.69 (m, 4H, H9 + H11 + H13); 7.17–7.07 (m, 6H, H8 + H6 + H12 + H14); 7.91 (d, 2H), 8.06 (d, 2H) ($H_{carboxylate\ ligand}$); 8.40 (s, 2H, H4); 10.10 (s, 1H, CHO). Single crystals of $\mathbf{1} \cdot 2H_2O \cdot 2.5DMSO$ suitable for X-ray diffraction studies were obtained by recrystallisation of the initial sample using DMSO.

The same complex was obtained if $Zn(acac)_2 \cdot yH_2O$, H_3L^1 and the acid were mixed in a 4 : 2 : 1 molar ratio.

$[Zn_2L^2(p\text{-}OOC–C_6H_4–CHO)] \cdot 2H_2O$. Yield: 0.38 g (65%), mp >300 °C. MS (ES): m/z 820.8 ($[Zn_2L^2]^+$), 994.6 ($[Zn_2L^2(OOC–C_6H_4–CHO)Na]^+$). ^{1}H NMR (300 MHz, DMSO-d_6): δ 2.83–2.62 (m, 6H), 3.38–3.30 (m, 2H), 3.53–3.52 (m, 2H), 3.77 (t, 2H) (H1 + H2 + H3); 4.19 (s, 1H, H17); 6.66–6.63 (m, 3H, H9 + H14); 7.29–7.18 (m, 5H, H6 + H8 + H13); 7.39 (s, 1H, H11); 7.91 (d, 2H), 8.05 (d, 2H) ($H_{carboxylate\ ligand}$); 8.36 (s, 2H, H4); 10.04 (s, 1H, CHO).

$[Zn_2L^1(o\text{-}OOC–C_6H_4–COOH)] \cdot 6H_2O$. Yield: 0.064 g (32%), mp >300 °C. MS (ES): m/z 587.1 ($[Zn_2L^1]^+$), 751.2 ($[Zn_2L^1(HOOC–C_6H_4–COOH)]^+$). ^{1}H NMR (300 MHz, DMSO-d_6): δ 2.59–2.53 (m, 4H), 3.70 (t, 2H), 3.98–3.91 (m, 6H) (H1 + H2 + H3); 4.02 (s, 1H, H17); 6.37 (t, 2H, H7); 6.76–6.67 (m, 4H, H9 + H11 + H13); 7.14–7.09 (m, 6H, H8 + H6 + H12 + H14); 7.37 (d, 2H), 7.58 (d, 2H) ($H_{carboxylate\ ligand}$); 8.22 (s, 2H, H4).

$[Zn_2L^2(o\text{-}OOC–C_6H_4–COOH)] \cdot 3H_2O$. Yield: 0.10 g (35%), mp >300 °C. MS (ES): m/z 822.8 ($[Zn_2L^2]^+$), 988.8 ($[Zn_2L^2(HOOC–C_6H_4–COOH)]^+$). ^{1}H NMR (300 MHz, DMSO-d_6): δ 2.84–2.70 (m, 6H), 3.75–3.58 (m, 4H, H1 + H2 + H3); 4.14 (s, 1H, H17); 6.53 (d, 1H, H14); 6.64 (d, 2H, H9); 7.25–7.19 (m, 5H, H8 + H6 + H13); 7.36 (s, 1H, H11); 7.46 (d, 2H), 7.76 (d, 2H) ($H_{carboxylate\ ligand}$); 8.26 (s, 2H, H4).

The complexes of $(Zn_2L^x)_2(OOC–C_1H_m–COO)$ stoichiometry were isolated by a similar method, exemplified by the preparation of $[(Zn_2L^1)_2(OOC–CH_2–COO)] \cdot 10H_2O$.

$[(Zn_2L^1)_2(OOC–CH_2–COO)] \cdot 10H_2O$. To a methanol solution (60 mL) of zinc acetylacetonate hydrate (0.31 g, 1.12 mmol) in a 100 mL round-bottomed flask were added H_3L^1 (0.27 g, 0.59 mmol) and acetonitrile (20 mL). The mixture was stirred until a yellow solution was obtained. Next, malonic acid (0.031 g, 0.29 mmol) was added and the flask equipped with a water-cooled condenser. The mixture was heated to reflux with stirring for 4 h, and the precipitated white–yellow solid was filtered off and dried in air. Yield: 0.3 g (71%),

mp >300 °C. MS (ES): *m*/*z* 587.2 ($[Zn_2L^1]^+$), 1275.3 ($[(Zn_2L^1)_2(OOC–CH_2–COOH)]^+$). ^{1}H NMR (300 MHz, DMSO-d_6): δ 2.41–2.34 (m, 4H), 2.52 (d, 4H), 3.39–3.35 (m, 4H), 3.58–3.42 (m, 12H) (H1 + H2 + H3 + –CH_2–); 3.98 (s, 2H, H17); 6.39 (t, 4H, H7); 6.67–6.64 (m, 8H, H9 + H12 + H14); 7.15–7.05 (m, 12H, H6 + H8 + H11 + H13); 8.29 (s, 4H, H4). ^{13}C NMR (300 MHz, DMSO-d_6): δ 47.2 (–CH_2–); 51.0, 54.9, 55.1 (C1 + C2 + C3); 90.6 (C17); 113.1, 118.4, 119.5, 122.2, 123.0, 124.3, 131.7, 132.9, 134.5, 135.9 (C5–C9 + C11–C14 + C16); 164.1, 171.6, 172.5 (C4 + C10 + C15); 175.2 (COO^-).

The same complex was obtained if $Zn(acac)_2 \cdot yH_2O$, H_3L^1 and the acid were mixed in a 2 : 1 : 1 molar ratio.

$[(Zn_2L^2)_2(OOC–CH_2–COO)] \cdot 6H_2O$. Yield: 0.29 g (71%), mp >300 °C. MS (ES): *m*/*z* 821.2 ($[Zn_2L^2]^+$), 1766.5 ($[(Zn_2L^2)_2(OOC–CH_2–COO)Na]^+$). ^{1}H NMR (300 MHz, DMSO-d_6): δ 2.47–2.43 (m, 4H), 2.59–2.52 (m, 8H), 3.58–3.50 (m, 8H) (H1 + H2 + H3 + –CH_2–); 4.06 (s, 2H, H17); 6.57 (d, 2H, H14); 6.65 (d, 4H, H9); 7.25–7.18 (m, 10H, H6 + H8 + H13); 7.35 (s, 2H, H11); 8.27 (s, 4H, H4). ^{13}C NMR (300 MHz, DMSO-d_6): δ 46.6 (–CH_2–); 51.1, 54.9, 55.1 (C1 + C2 + C3); 89.4 (C17); 102.7, 110.5, 120.0, 124.3, 125.4, 126.6, 134.5, 135.1, 136.7, 137.1 (C5–C9 + C11–C14 + C16); 163.5, 170.8, 171.24 (C4 + C10 + C15); 175.4 (COO^-).

$[(Zn_2L^1)_2(OOC–CH_2CH_2–COO)] \cdot 4.25H_2O$ ($2 \cdot 4.25H_2O$). Yield: 0.29 g (38%), mp >300 °C. MS (ES): *m*/*z* 589.0 ($[Zn_2L^1]^+$), 1288.0 ($[(Zn_2L^1)_2(OOC–CH_2–COO)Na]^+$). ^{1}H NMR (300 MHz, DMSO-d_6): δ 2.48 (s, 4H, –CH_2– acid); 2.54–2.51 (m, 2H), 2.66–2.60 (m, 8H), 3.32–3.27 (m, 4H), 3.48–3.40 (m, 4H), 3.65 (t, 4H) (H1 + H2 + H3); 4.04 (s, 2H, H17); 6.38 (t, 4H, H7); 6.75–6.69 (m, 8H, H9 + H12 + H14); 7.15–7.03 (m, 12H, H6 + H8 + H11 + H13); 8.28 (s, 4H, H4). ^{13}C NMR (300 MHz, DMSO-d_6): δ 32.9 (–CH_2–); 50.4, 54.2, 54.4 (C1 + C2 + C3); 89.6 (C17); 112.5, 117.7, 118.9, 121.5, 122.3, 123.7, 131.1, 132.4, 133.9, 135.3 (C5–C9 + C11–C14 + C16); 163.3, 171.0, 171.7 (C4 + C10 + C15); 180.2 (COO^-).

Single crystals of $[(Zn_2L^1)_2(OOC–CH_2CH_2–COO)] \cdot 4.25H_2O \cdot 0.75MeOH \cdot 0.5MeCN$ ($\mathbf{2} \cdot 4.25H_2O \cdot 0.75MeOH \cdot 0.5MeCN$) were isolated by slow evaporation of the reaction solution. The elemental analysis was in agreement with the formulation $[(Zn_2L^1)_2(OOC–CH_2CH_2–COO)] \cdot 4.25H_2O$, showing that the sample loses the most volatile solvents upon drying.

$[(Zn_2L^2)_2(OOC–CH_2CH_2–COO)] \cdot 5H_2O$ ($\mathbf{3} \cdot 5H_2O$). Yield: 0.37 g (36%), mp >300 °C. MS (ES): *m*/*z* 822.8 ($[Zn_2L^2]^+$), 1782.6 ($[(Zn_2L^2)_2(OOC–CH_2–COO)Na]^+$). ^{1}H NMR (300 MHz, DMSO-d_6): δ 2.47 (s, 4H, –CH_2– acid); 2.59–2.51 (m, 4H), 2.71–2.64 (m, 8H), 3.35–3.38 (m, 4H), 3.46–3.41 (m, 4H), 3.66 (t, 4H) (H1 + H2 + H3); 4.11 (s, 2H, H17); 6.61 (d, 2H, H14); 6.64 (d, 4H, H9); 7.25–7.20 (m, 10H, H6 + H8 + H13); 7.36 (s, 2H, H11); 8.29 (s, 4H, H4). ^{13}C NMR (300 MHz, DMSO-d_6): δ 32.8 (–CH_2–); 50.5, 54.2, 54.4 (C1 + C2 + C3); 88.4 (C17); 102.2, 110.1, 119.3, 123.6, 124.6, 126.0, 133.8, 136.1, 136.5 (C5–C9 + C11–C14 + C16); 162.6, 170.2, 170.4 (C4 + C10 + C15); 180.3 (COO^-).

Single crystals of $[(Zn_2L^2)_2(OOC–CH_2CH_2–COO)] \cdot 7H_2O \cdot 0.25MeOH$ ($\mathbf{3} \cdot 7H_2O \cdot 0.25MeOH$) were isolated by slow evaporation of the reaction solution. The elemental analysis was in agreement with the formulation $[(Zn_2L^2)_2(OOC–CH_2CH_2–COO)] \cdot 5H_2O$, showing that the crystalline sample loses methanol and some water upon drying.

$[(Zn_2L^1)_2(p\text{-}OOC–C_6H_4–COO)] \cdot 11H_2O$ ($\mathbf{4} \cdot 11H_2O$). Yield: 0.64 g (41%), mp >300 °C. MS (ES): *m*/*z* 587.2 ($[Zn_2L^1]^+$), 1335.2 ($[(Zn_2L^1)_2(p\text{-}OOC–C_6H_4–COOH)]^+$). ^{1}H NMR (300 MHz, DMSO-d_6): δ 2.80–2.55 (m, 12H), 3.40–3.31 (m, 4H), 3.54–3.46 (m, 4H), 3.75 (4H, t) (H1 + H2 + H3); 4.12 (s, 2H, H17); 6.38 (t, 4H, H7); 6.80–6.68 (m, 8H, H9 + H12 + H14); 7.17–7.05 (m, 12H, H8 + H6 + H11 + H13); 7.93 (s, 4H, $H_{carboxylate\ ligand}$); 8.34 (s, 4H, H4).

Single crystals of $[(Zn_2L^1)_2(p\text{-}OOC–C_6H_4–COO)] \cdot 2.5H_2O \cdot MeOH \cdot 6EtOH$ ($\mathbf{4} \cdot 2.5H_2O \cdot MeOH \cdot 6EtOH$) were obtained by recrystallising the bulk sample $[(Zn_2L^1)_2(p\text{-}OOC–C_6H_4–COO)] \cdot 11H_2O$ from methanol/ethanol.

$[(Zn_2L^2)_2(p\text{-}OOC–C_6H_4–COO)] \cdot 2H_2O$. Yield: 0.34 g (54%), mp >300 °C. MS (ES): *m*/*z* 821.1 ($[Zn_2L^2]^+$), 1829.6 ($[(Zn_2L^2)_2(OOC–C_6H_4–COO)Na]^+$). ^{1}H NMR (300 MHz, DMSO-d_6): δ 2.85–2.58 (m, 12H), 3.39–3.29 (m, 4H), 3.54–3.45 (m, 4H), 3.75 (t, 4H) (H1 + H2 + H3); 4.18 (s, 2H, H17); 6.66–6.60 (m, 6H, H9 + H14); 7.20 (d, 4H, H8); 7.29–7.23 (m, 6H, H6 + H11); 7.38 (d, 2H, H13); 7.90 (s, 4H, $H_{carboxylate\ ligand}$); 8.34 (s, 4H, H4).

Spectrophotometric and spectrofluorimetric measurements

Absorption spectra were recorded on a Perkin-Elmer Lambda 35 spectrophotometer, and fluorescence emission spectra on Perkin-Elmer LS45 and Horiba-Jobin Yvon-Spex Fluorolog 3.22 spectrofluorimeters. The linearity of the fluorescence emission *vs*. concentration was checked in the concentration range used (10^{-4}–10^{-6} M). A correction for absorbed light was performed when necessary. The spectrofluorimetric titrations were performed as follows. Stock solutions of the ligands (*ca*. 10^{-3} M) were prepared by dissolving an appropriate amount of the ligand in a 50 mL volumetric flask and diluting it to the mark with DMSO (UVA-sol or HPLC grades) or a 10/90 v/v mixture of DMSO/ethanol. Titration solutions were prepared by the appropriate dilution of the stock solutions to 10^{-5} and 10^{-6} M. Titrations of both ligands were carried out by the addition of μL amounts of standard solutions of Zn(II) ions in DMSO or absolute ethanol. The metal salts $Zn(NO_3)_2$ and $Zn(CF_3SO_3)_2$ were commercial products (from Aldrich) and were used without further purification.

Fluorescence spectra of solid samples were recorded using the spectrofluorimeter, exciting the solid compounds at appropriate wavelengths (nm). Emission spectra were recorded in the 300–500 nm range using a fiber optic system connected to the Horiba-Jobin Yvon-Spex Fluorolog 3.22 spectrofluorimeter.

Luminescence quantum yields were measured using a solution of quinine sulfate in sulfuric acid (0.1 M) as a standard (Φ_F = 0.54),[22] and were corrected for the different refraction indices of the solvents.[23]

In all fluorimetric measurements, the optical density of the solution did not exceed 0.1.

Crystallography

Single crystals of $\mathbf{1}\cdot 2H_2O\cdot 2.5DMSO$, $\mathbf{2}\cdot 4.25H_2O\cdot 0.75MeOH\cdot 0.5MeCN$, $\mathbf{3}\cdot 7H_2O\cdot 0.25MeOH$ and $\mathbf{4}\cdot 2.5H_2O\cdot MeOH\cdot 6EtOH$ were obtained as detailed above. Diffraction data were collected at 100 K using Bruker SMART CCD-1000 or Bruker X8 Kappa APEXII diffractometers by employing graphite-monochromated Mo-K_α radiation (λ = 0.71073 Å). Data were processed and corrected for Lorentz and polarisation effects. A multi-scan absorption correction was applied using SADABS.[24] The structures were solved by direct methods using SIR-92[25] and refined by full matrix least-squares on F^2 using the SHELXL-97[26] program package. Non-hydrogen atoms were anisotropically refined, except for some solvate atoms, which were disordered or had low partial occupation sites. Hydrogen atoms were included by employing a riding model, except for those attached to water molecules, which were located on Fourier maps, fixed and given isotropic displacement parameters of 0.08 $Å^2$, or depending on the parent atoms. Partial occupancies of solvate molecules were individually refined and then rounded to simplify the formulae.

Crystallographic data (excluding structure factors) for the structures reported in this paper have been deposited with the Cambridge Crystallographic Data Centre.‡

Acknowledgements

The authors thank Xunta de Galicia (PGIDTIT06PXIB209043PR) and the Portuguese Foundation for Science and Technology (POCI/QUI/55519/2004 FCT/FEDER) for financial support.

References

1 T. Bark, M. Düggeli, H. Stoeckli-Evans and A. von Zelewsky, *Angew. Chem., Int. Ed.*, 2001, **40**, 2848.
2 A. Zimmer, D. Kuppert, T. Weyhermüller, I. Müller and K. Hegetschweiler, *Chem.–Eur. J.*, 2001, **7**, 917.
3 T.-L. Hu, J.-R. Li, C.-S. Liu, X.-S. Shi, J.-N. Zhou, X.-H. Bu and J. Ribas, *Inorg. Chem.*, 2006, **45**, 162.
4 B.-H. Ye, X.-Y. Li, I. D. Willliams and X.-M. Chen, *Inorg. Chem.*, 2002, **41**, 6426.
5 (*a*) D. Visinescu, M. Andruh, A. Muller, M. Schmidtmann and Y. Journaux, *Inorg. Chem. Commun.*, 2002, **5**, 42; (*b*) D. Visinescu, G. I. Pascu, M. Andruh, J. Magull and H. W. Roesky, *Inorg. Chim. Acta*, 2002, **340**, 201; (*c*) D. Visinescu, A. M. Madalan, V. Kravtsov, Y. A. Simonov, M. Schmidtmann, A. Muller and M. Andruh, *Polyhedron*, 2003, **22**, 1385.
6 (*a*) M. Pascu, M. Andruh, A. Mueller and M. Schmidtmann, *Polyhedron*, 2004, **23**, 673; (*b*) M. Pascu, F. Lloret, N. Avarvari, M. Julve and M. Andruh, *Inorg. Chem.*, 2004, **43**, 5189; (*c*) R. Gheorghe, P. Cucos, M. Andruh, J.-P. Costes, B. Donnadieu and S. Shova, *Chem.–Eur. J.*, 2006, **12**, 187.
7 (*a*) P. Braunstein and F. Naud, *Angew. Chem., Int. Ed.*, 2001, **40**, 680; (*b*) C. Gambs, S. Chaloupka, G. Consiglio and A. Togni, *Angew. Chem., Int. Ed.*, 2000, **39**, 2486.
8 I. Bertini, H. B. Gray, S. J. Lippard and J. S. Valentine, *Bioinorganic Chemistry*, University Science Books, California, 1994.
9 D. E. Fenton, *Chem. Soc. Rev.*, 1999, **28**, 159.
10 R. E. P. Winpenny, *Adv. Inorg. Chem.*, 2001, **52**, 1.
11 (*a*) M. Fondo, A. M. García-Deibe, M. R. Bermejo, J. Sanmartín and A. L. Llamas-Saiz, *J. Chem. Soc., Dalton Trans.*, 2002, 4746; (*b*) M. Fondo, A. M. García-Deibe, J. Sanmartín, M. R. Bermejo, L. Lezama and T. Rojo, *Eur. J. Inorg. Chem.*, 2003, 3703; (*c*) M. Fondo, A. M. García-Deibe, M. Corbella, J. Ribas, A. Llamas-Saiz, M. R. Bermejo and J. Sanmartín, *Dalton Trans.*, 2004, 3503; (*d*) M. Fondo, A. M. García-Deibe, N. Ocampo, M. R. Bermejo and J. Sanmartín, *Dalton Trans.*, 2004, 2135.
12 S. Kitagawa, R. Kitaura and S. Noro, *Angew. Chem., Int. Ed.*, 2004, **43**, 2334.
13 A. D. Burrows, R. W. Harrington, M. F. Mahon and S. J. Teat, *Cryst. Growth Des.*, 2004, **4**, 813.
14 C. N. R. Rao, S. Natarajan and R. Vaidhyanathan, *Angew. Chem., Int. Ed.*, 2004, **43**, 1466.
15 (*a*) B.-H. Ye, X.-Y. Li, I. D. Willliams and X.-M. Chen, *Inorg. Chem.*, 2002, **41**, 6426; (*b*) B.-H. Ye, M.-L. Tong and X.-M. Chen, *Coord. Chem. Rev.*, 2005, **249**, 545.
16 A. W. Addison, T. N. Rao, J. Reedijk, J. van Rijn and G. C. Verschoor, *J. Chem. Soc., Dalton Trans.*, 1984, 1349.
17 L.-W. Yang, S. Liu, E. Wong, S. J. Rettig and C. Orvig, *Inorg. Chem.*, 1995, **34**, 2164.
18 E. Pretsch, T. Clerc, J. Seibl and W. Simon, *Tables of Spectral Data for Structure Determination of Organic Compounds*, Springer-Verlag, Berlin, 2nd edn., 1989.
19 (*a*) L. Biczók, T. Bérces and H. Inoue, *J. Phys. Chem. A*, 1999, **103**, 3837; (*b*) M. Vicente, R. Bastida, C. Lodeiro, A. Macías, A. J. Parola, L. Valencia and S. E. Spey, *Inorg. Chem.*, 2003, **42**, 6768.
20 (*a*) H. D. Burrows, S. J. Formosinho and M. F. J. R. Paiva, *J. Photochem.*, 1980, **12**, 285; (*b*) D. A. R. Rubio, D. Zanette, F. Nome and C. A. Bunton, *Langmuir*, 1994, **10**, 1151.
21 (*a*) W. S. Kim, J. M. You, B. J. Lee, Y. K. Jang, D. E. Kim and Y. S. Kwon, *J. Nanosci. Nanotechnol.*, 2006, **6**, 3637; (*b*) W. L. Jia, D. R. Bai, T. McCormick, Q. D. Lius, M. Motala, R. Y. Wang, C. Seward, Y. Tao and S. M. Wang, *Chem.–Eur. J.*, 2004, **10**, 994; (*c*) P. F. Wang, Z. R. Hong, Z. Y. Xie, S. W. Tong, O. Y. Wong, C. S. Lee, N. B. Wong, L. S. Hung and S. T. Lee, *Chem. Commun.*, 2003, 1664; (*d*) E. M. Gross, J. D. Anderson, A. F. Slaterbeck, S. Thayumanavan, S. Barlow, Y. Zhan, S. R. Marder, H. K. Hall, M. F. Nabor, J. F. Wang, E. A. Mash, N. R. Amstrong and R. M. Wightman, *J. Am. Chem. Soc.*, 2000, **122**, 4972.
22 I. B. Berlman, *Handbook of Fluorescence Spectra of Aromatic Molecules*, Academic Press, New York, 2nd edn., 1971.
23 J. R. Lakowicz, *Principles of Fluorescence Spectroscopy*, Springer Science, New York, 2nd edn., 1999.
24 (*a*) G. M. Sheldrick, *SADABS: Program for area detector adsorption correction*, Institute for Inorganic Chemistry, University of Göttingen, Germany, 1996; (*b*) R. H. Blessing, *Acta Crystallogr., Sect. A: Fundam. Crystallogr.*, 1995, **51**, 33.
25 *SIR-92: A program for crystal structure solution*: A. Altomare, G. Cascarano, C. Giacovazzo and A. Guagliardi, *J. Appl. Crystallogr.*, 1993, **26**, 343.
26 (*a*) G. M. Sheldrick, *SHELXS-97: Program for solution of crystal structures*, University of Göttingen, Germany, 1997; (*b*) G. M. Sheldrick, *SHELXL-97: Program for refinement of crystal structures*, University of Göttingen, Germany, 1997.